

# Enhancing the Separation and Quantification of Perfluoroalkyl Substances Using Polymeric Ionic Liquid Sorbents in Thin Film Microextraction

Aghogho A. Olomukoro, Derek R. Eitzmann, Jared L. Anderson, and Emanuela Gionfriddo\*



Cite This: *Anal. Chem.* 2025, 97, 7610–7615



Read Online

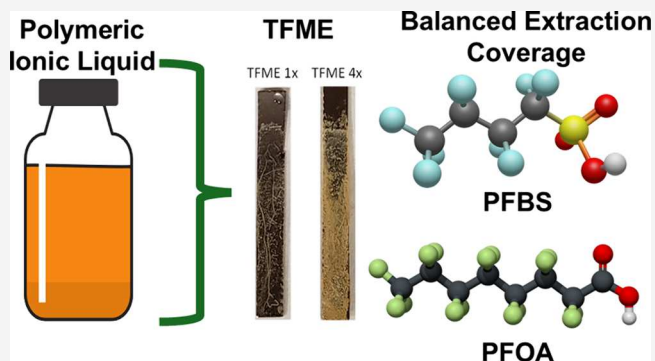
ACCESS |

Metrics & More

Article Recommendations

Supporting Information

**ABSTRACT:** The preconcentration and isolation of per- and polyfluoroalkyl substances (PFAS) remain challenging due to their varying chain lengths and diverse headgroup chemical functionalities. These substances are persistent and occur in the environment at low parts-per-trillion concentration levels, necessitating the use of efficient and selective sorbents that can enhance their preconcentration from the targeted sample prior to instrumental analysis. This study, for the first time, evaluates the use of a polymeric ionic liquid (PIL) consisting of 1-(9-carboxynonyl)-3-vinylimidazolium bromide [ $C_9COOHVim^+$ ] [ $Br^-$ ] ionic liquid (IL) monomer and 1,12-di(3-vinylimidazolium)dodecane bromide ( $[C_{12}(Vim^+)_2]2[Br^-]$ ) IL cross-linker for the simultaneous separation and preconcentration of 15 anionic PFAS. The PIL was immobilized on a thin film microextraction device to improve preconcentration, extraction, and desorption kinetics. The addition of competing anions to the desorption solution was critical to ensure the quantitative desorption of the anionic PFAS by an ion exchange mechanism. Partition coefficient calculations revealed a balanced extraction coverage for short- and long-chain PFAS in ultrapure water, while in solutions at high ionic strength, short-chain PFAS tend to display less affinity for the sorbent compared to long-chain PFAS. Kinetic studies showed that less hydrophobic PFAS (perfluorobutanoic acid (PFBA)–perfluorohexanoic acid (PFHxA)) reached equilibrium faster and the extraction followed a pseudo-second order model with  $r^2$  values up to 0.9874. The applicability of the PIL-thin film microextraction (TFME) device for quantitative analysis was demonstrated by a calibration curve in a concentration range from 1 ng L<sup>-1</sup> to 2500 ng L<sup>-1</sup>, which showed good accuracy (70–130%), precision (<20%), and limits of quantification from 1 ng L<sup>-1</sup> to 50 ng L<sup>-1</sup>.



## INTRODUCTION

Ionic liquids (ILs) are effective sorbents for the extraction of various environmental contaminants, including pesticides,<sup>1,2</sup> phthalate esters,<sup>3,4</sup> and polyaromatic hydrocarbons (PAHs).<sup>5–7</sup> ILs are organic molten salts with melting points below 100 °C and usually consist of a bulky organic nitrogen cation such as imidazolium, pyridinium, pyrrolidinium, phosphonium, or ammonium and an organic (trifluoromethylsulfonate [ $CF_3SO_3^-$ ], bis[(trifluoromethyl)sulfonyl]imide [ $NTf_2^-$ ], trifluoroethanoate [ $CF_3CO_2^-$ ]) or inorganic ( $Cl^-$ ,  $PF_6^-$ ,  $BF_4^-$ ) halogen-based anion.<sup>8</sup> The choice of cation and anion components plays a crucial role in ILs physicochemical properties, which allows their easy tunability for efficient isolation, preconcentration, and separation of molecules with diverse chemistries. ILs have shown potential for isolating per- and polyfluoroalkyl substances (PFAS), a class of anthropogenic chemicals highly monitored in environmental and biological samples and pharmaceutical formulations due to their ubiquitous presence and potential effects on human health.<sup>9,10</sup> The extensive use of PFAS in the manufacturing

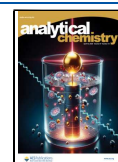
industry within the past six decades has led to their uncontrolled discharge in the environment, where they have been found to be extremely persistent and mobile, resulting in documented bioaccumulation in biota and consequent biomagnification at different trophic levels.<sup>11,12</sup> Therefore, PFAS isolation and preconcentration for remediation and analytical purposes are of utmost importance, especially for mixtures that include PFAS with varied alkyl chain lengths and functionalities of the headgroup moieties. Dong et al.<sup>13</sup> investigated the modification of clay with imidazolium-based ILs for the sorption of perfluorooctanoic acid (PFOA) and perfluorooctanesulfonate (PFOS). The results showed that the IL-modified clay with a longer alkyl chain had the highest

**Received:** December 2, 2024

**Revised:** March 18, 2025

**Accepted:** March 24, 2025

**Published:** April 7, 2025



removal efficiency for both PFOA and PFOS. Chen et al.<sup>14</sup> immobilized a polymeric ionic liquid (PIL) on an anodized Ti wire to create a solid phase microextraction (SPME) fiber for the removal of six anionic PFAS compounds from aqueous solution. A comparison with other commonly used SPME extraction phases showed that the new PIL coating exhibited higher extraction efficiency, selectivity, and stability. More recently, Eitzmann et al.<sup>15,16</sup> immobilized IL on thin film microextraction (TFME) devices for the preconcentration and isolation of DNA. The results demonstrated the significance of ions in an aqueous solution for the desorption of DNA from these ionic sorbents to exchange the negatively charged phosphodiester backbone from the polycationic moiety. While a concentrated salt solution was crucial for successful DNA desorption, high ionic strength solutions hindered downstream applications. Therefore, different salts and their concentrations were tested to maximize the enrichment factor and ensure effective DNA desorption with minimal amounts of salt. Given these applications, in this study, a PIL thin film device, consisting of the IL monomer 1-(9-carboxy-nonyl)-3-vinylimidazolium bromide [ $C_9COOHVim^+$ ] [ $Br^-$ ] and the IL cross-linker 1,12-di(3-vinylimidazolium)dodecane bromide ( $[C_{12}(Vim^+)_2]_2[Br^-]$ ), previously investigated by Eitzmann et al.<sup>16</sup> for DNA applications, was used for the simultaneous preconcentration of 15 negatively ionic PFAS from aqueous solutions. The desorption conditions were tuned to be compatible with liquid chromatography–mass spectrometry (LC-MS). The addition of ammonium salts to the desorption solution was crucial to enable quantitative desorption and compatibility with LC-MS. The use of the PIL in a thin film geometry for microextraction (i.e., TFME) was instrumental in enhancing the extraction efficiency and improving the analysis throughput. These are crucial factors, given the low concentrations of PFAS in environmental samples. The combination of PILs and TFME overcomes challenges related to extracting PFAS mixtures with conventional sorbent materials, by providing a balanced extraction coverage for PFAS with varied chemistries.<sup>17,18</sup>

## MATERIALS AND METHODS

A detailed description of the standards and other reagents used in this work can be found in the [Supporting Information](#) (Section S1-Materials). Preparation of the TFME devices was performed according to a protocol proposed by Eitzmann et al.<sup>15,16</sup> ([Supporting Information](#), Section S2-Preparation of the TFME devices). Liquid chromatography and mass spectrometry conditions are discussed in [Supporting Information](#), Section S3.

**TFME Procedure.** Newly prepared TFME devices were thoroughly cleaned in ultrapure water to remove excess photoinitiator before use. Subsequently, the thin films were conditioned in a saturated NaCl solution until extraction. Regeneration of the PIL was performed after every extraction-desorption step by placing the thin films in saturated NaCl. Prior to extraction, the devices were rinsed with ultrapure water; the rinsing procedure was found to be critical in avoiding any NaCl to be retained on the device, resulting in contamination of the sample. Extraction was performed in a 2 mL glass vial with a sample volume of 1.75 mL for 30 min. A 700  $\mu$ L plastic vial was used for desorption with 700  $\mu$ L of desorption solution of 2% (w:v) ammonium formate in 80:20 MeOH:H<sub>2</sub>O (v:v). Both extraction and desorption were performed with agitation at 1000 rpm. Special considerations

on cleaning procedures to be performed on the devices for first use after synthesis are reported in [Supporting Information](#), Section 4-Preparing the TFME devices for first use. Interaction of the PFAS compounds with the PIL sorbent was further investigated using kinetic models as described in [Supporting Information](#), Section 5-Kinetic models.

**Method Validation.** A calibration curve was performed to determine the suitability of this PIL-TFME device for the quantification of parts per trillion (ppt) concentrations of PFAS. Method validation was performed by spiking ultrapure water at different concentrations, namely 50, 100, 150, 250, 500, 1000, 5000, and 10000 ng L<sup>-1</sup> with internal standard concentration at 750 ng L<sup>-1</sup>. Interday and intraday studies were performed at concentration levels of 75, 300, 750, and 3000 ng L<sup>-1</sup> and were assessed over 1 week. To determine the limits of quantification (LOQs) and detection (LODs), lower concentration levels were prepared at 1, 2.5, 5, 10, 20, 50, 100, 250, 500, 1000, and 2500 ng L<sup>-1</sup> and internal standards spiked at 150 ng L<sup>-1</sup> (note: concentration values indicate individual levels of PFAS analytes and internal standards). The LOQs were determined based on the lowest calibration curve concentration level that met accuracy between 70% and 130% with precision  $\leq 20\%$ .<sup>19,20</sup> Samples at each concentration level were prepared in triplicate and extracted independently; each desorption solution obtained was injected into the instrument three times, yielding a total of nine replicate measurements for each concentration level.

## RESULTS AND DISCUSSION

**Desorption Conditions.** Optimal desorption is crucial for SPME method development as inadequate protocols can bias analyte quantification. Residual analytes on the sorbent may compromise the accuracy of the results and the device reusability. Selecting the appropriate desorption conditions is also key to robust chromatography and avoiding mobile phase mismatches that result in distorted chromatographic peaks. Our previous studies<sup>21,22</sup> highlighted the role of ammonium salts in minimizing the percent carryover of PFAS on ion-exchange extraction phases. Since the PIL contains cationic moieties and anions, it was necessary to understand how the removal of PFAS is influenced by the presence of competing salts and how PFAS can be quantitatively and efficiently desorbed. In this study, we investigated the desorption mechanism of PFAS from the PIL extraction phase with 2% (v:v or w:v) ammonium hydroxide, ammonium chloride, and ammonium formate in the desorption solution. Adding the ammonium salts reduced the percentage of PFAS retained on the sorbent, with ammonium formate promoting the most efficient desorption ([Figure S1](#)). [Figure 1](#) shows that the PFAS desorption from the PIL was inefficient without ammonium salts in the desorption solution. This is due to strong interactions between negatively charged PFAS and the ionic sorbent, requiring counterions to enable effective desorption. While NaCl was previously used for efficient DNA desorption from PILs,<sup>16</sup> this study opted for ammonium salts due to their superior compatibility with LC-MS. The TFME devices with 4 $\times$  thickness had a higher percent carryover than those with 1 $\times$  due to the thicker extraction phase. More considerations about the device thickness and rationale for selecting the 1 $\times$  TFME for further studies are presented in [Supporting Information](#) Section 6-PIL coating thickness. PFBS and PFOS, the two sulfonate PFAS studied, showed higher carryover than carboxylate PFAS (<2%) when ammonium

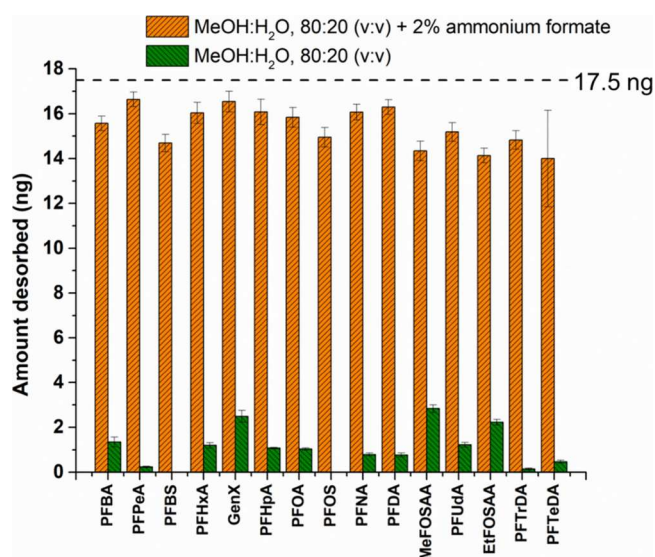


**Figure 1.** Desorption of PFAS with and without ammonium formate in an 80:20 MeOH:H<sub>2</sub>O (v:v) desorption solution. Extraction and desorption times were 90 min at 1000 rpm. The individual concentration of PFAS in the 1.75 mL ultrapure water sample was 10  $\mu\text{g L}^{-1}$ , resulting in 17.5 ng of each PFAS spiked in the sample.

formate and ammonium chloride were used in the desorption solution, respectively, 7.1% and 7.8% (Figure S2). This higher carryover likely results from sulfonate groups forming stronger ion pairs with the imidazolium cation than carboxylate groups, leading to less efficient desorption.<sup>8,23</sup> Another interesting observation was that the desorption efficiency of PFBS and PFOS was lower when ammonium hydroxide (3.5 and 2.9 ng) was added to the desorption solution compared to ammonium formate (15.5 and 14.9 ng) and ammonium chloride (13.8 and 13.9 ng). This trend may be explained by the hydroxide ion having a lower tendency to pair with the imidazolium cation, resulting in the lowest desorption efficiency.<sup>24</sup>

From the desorption time profile shown in Figure S3, 10 min was chosen as the optimized desorption time to ensure quantitative desorption and reproducibility.

#### Effect of Dissolved Ions on PFAS Extraction Efficiency.

Understanding how different physiochemical conditions affect PFAS isolation and separation is critical for predicting molecular mechanisms that govern sorption processes in real samples for both analytical extractions and remediation purposes. The extraction efficiency of PFAS can be affected by coexisting ions in solution, as they can compete with PFAS for interaction with the ion exchange moieties in the PIL extraction phase. Understanding the link between the sorption efficiency of PFAS at varying ionic strength of the sample elucidates their partitioning behavior in various complex systems such as air–water, soil–water, and non-aqueous liquid–water interfaces, which is relevant to PFAS fate and transport.<sup>25</sup> This study used simulated seawater to test the effect of codissolved ions in an aqueous solution of PFAS on extraction efficiency. The seawater was then diluted to different concentrations to simulate the ionic strength of different aquatic systems.<sup>26,27</sup> Details of the dilutions and concentration values can be found in the Supporting Information (Table S1). The results showed that the amount of PFAS extracted decreased as ionic strength increased (Figure 2). In particular, for short-chain PFAS, Perfluorobutanoic acid (PFBA)–perfluorohexanoic acid (PFHxA) (except PFBS), there was a

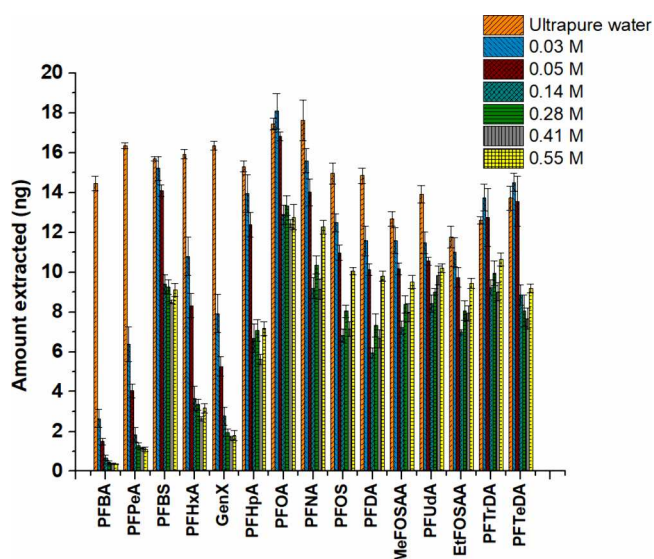


**Figure 2.** Effect of the ionic strength of PFAS extraction evaluation using simulated seawater containing different salt compositions. Extraction and desorption were performed at 90 min at 1000 rpm.

significant decrease in extraction efficiency when the ionic strength was increased to 0.03 M. The higher ionic strength increased the available ions in solution, potentially promoting competitive sorption with PFAS resulting in decreased extraction efficiency, especially for short-chain PFAS. Co-dissolved ions in solution can, in fact, shield ionic interactions with the sorbent, hindering the short-chain PFAS from undergoing electrostatic attraction with the PIL polymer.<sup>8</sup> Other studies have observed similar behavior with various sorbents (particularly cationic sorbents), where potential competition between PFAS and other ions in the solution occurs at a high ionic strength resulting in decreased extraction efficiency.<sup>28–30</sup> In contrast, longer-chain PFAS (PFNA–PFTeDA) showed a less pronounced decrease in the extraction efficiency, likely due to stronger hydrophobic interactions with the sorbent. This result emphasizes the dominance of hydrophobic interaction for the sorption of bulkier PFAS.<sup>28</sup> Interestingly, ionic strength had a notable impact on the extraction of PFBA and PFBS, both of which possess a C4 chain but differ in their headgroups—carboxylate and sulfonate, respectively. Similar to long-chain PFASs, PFBS was less affected by increasing ionic strength. This behavior may be explained by the antipolyelectrolyte effect, a phenomenon observed in polymers containing both anionic and cationic groups, which leads to enhanced polymer hydration at higher salt concentrations. Previous studies have demonstrated that this effect depends on the specific type of anion water affinity as well as its concentration.<sup>31</sup> It is understood that ammonium cations and sulfonate anions offer a better match to water affinities than carboxylate, hence contributing to a significant decrease in extraction efficiency in the presence of high ionic strength for PFBA compared to PFBS.<sup>15</sup>

In addition to ionic strength affecting extraction efficiency, the pH of the solution is also critical for the effective adsorption of PFAS as it can influence the surface charge of the sorbents, which can be protonated only at certain pH values.<sup>32,33</sup> pH studies can be performed with either buffers or strong acid and base solutions. In this study, both approaches were used to assess whether comparable results

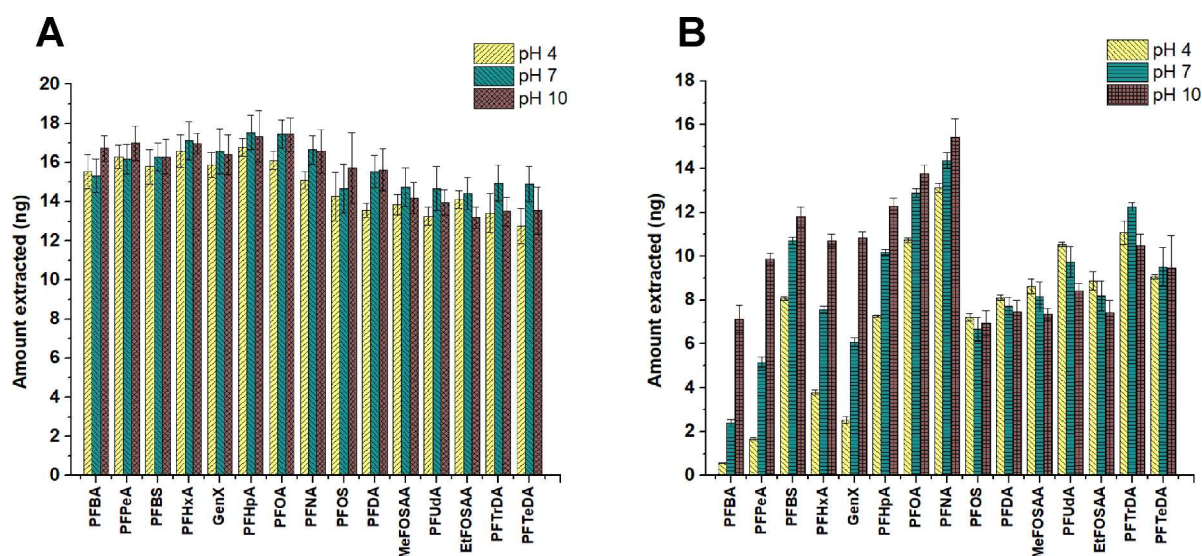


**Figure 3.** pH evaluation using (A) ultrapure water adjusted to pH 4, 7, and 10 with HCl or NaOH and (B) pH buffer solutions at pH 4, 7, and 10. Extraction and desorption steps were performed for 90 min with an agitation of 1000 rpm. The final concentration of individual PFAS in ultrapure water was  $10 \mu\text{g L}^{-1}$ .

could be achieved with the PIL. Although the employed PIL is a strong anion exchange sorbent (SAX), as it remains positively charged under all pH ranges, commercial buffer solutions with different pH values (e.g., 4, 7 and 10) were used to better understand the effect of coexisting electrolytes in solution (Figure 3). PFBA to PFNA displayed lower sorption at a buffer solution pH of 4, with sorption gradually increasing as the pH increased to 10. The salts present in the pH 4 buffer (sodium dihydrogen citrate; disodium hydrogen citrate; sodium chloride) contributed to the low recovery of these compounds with the PIL. The buffer at pH 7 contained potassium sodium phosphate, and the buffer at pH 10 was composed of disodium tetraborate/sodium hydroxide. The bulkier and more hydrophobic PFAS (PFOS–PFTeDA) exhibited a constant extraction efficiency over the investigated pH range and showed a weaker pH dependence when extracted in the presence of other ions. Since the exact concentrations of the salts in the buffers are proprietary, it is difficult to draw conclusions. However, from these results, it can be deduced that the ionic strength of the buffer solution affects the extraction efficiency of the shorter-chain PFAS more than their longer-chain counterparts, as observed in Figure 2. The evaluation of pH on extraction efficiency was also performed by adjusting the pH of ultrapure water to values of 4, 7, and 10 with sodium hydroxide (NaOH) and hydrochloric acid (HCl) to minimize the presence of diverse background electrolytes. These experiments revealed that PFAS showed similar extraction efficiencies at the pH values tested. According to simulations performed using the ChemAxon platform, the imidazolium moiety of the studied PIL sorbent is positively charged across all pH ranges, while the carboxylic acid moiety of the substituent group is negatively charged above pH 6 (Figure S4). It is noteworthy that, despite the presence of a negatively charged functional group, the extraction efficiency of PFAS was not affected. Both electrostatic and hydrophobic interactions were found to be effective in PFAS extraction, providing an advantage over WAX sorbents. In the case of WAX sorbents, the extraction efficiency is pH dependent, particularly for short-chain PFAS, where electrostatic interactions are the primary mechanism of interaction.<sup>21,22</sup>

**Extraction Time and Kinetics.** The extraction time and kinetics of PFAS sorption in the PIL sorbent were studied. Equilibrium was reached within 20–30 min for most PFAS (PFBA–PFNA) but took 60 min for more hydrophobic compounds (MeFOSAA to PFTeDA) (Figure S5). The longer equilibration time for long chain PFAS suggests steric hindrance affects their diffusion through the aqueous boundary layer and in the sorbent compared to the shorter chain and less hydrophobic PFAS.<sup>13</sup> Therefore, 30 min was selected as the optimal extraction time, although longer times can be considered to achieve higher recoveries for long-chain PFAS.

Kinetic modeling was applied to further understand the kinetic mechanism of the PFAS compounds. Pseudo-second order was observed to be the best fit for all analytes as shown in Figure S6 and Table S2. MeFOSAA and PFUdA provided the lowest  $r^2$  values, 0.8855 and 0.8586, respectively, compared to other analytes. This model indicates the presence of chemical adsorption, which is the interaction between the analytes and the sorbent, with the sorption rate being dependent on the available sites of the PIL sorbent.<sup>13</sup> In addition to the  $r^2$  value, the  $q_e$  values calculated were close to the experimental  $q_e$  value except for the later eluting analytes (for example, PFTeDA ( $q_e$  cal (0.0198) and  $q_e$  exp (0.0119)). The  $K_2$  values indicate that PFTtDA (1.63) and PFTeDA (0.76) reach saturation faster and therefore take longer to attain equilibrium compared to the short-chain PFAS. In addition to PSO, the intraparticle diffusion model (Table S3) also showed a good fit for the last 5 eluting analytes (MeFOSAA to PFTeDA) describing a multistage absorption process for these hydrophobic PFAS.<sup>34</sup> Pseudo-first order was evaluated, and poor  $r^2$  and  $q_e$  values were determined for all analytes, indicative that this model is not able to describe the kinetic behavior of PFAS on the PIL sorbent (Table S4).

**Partition Coefficient ( $K_{fs}$ ) and Thermodynamic Parameters.** The partition coefficient of PFAS between the PIL phase and aqueous media and simulated seawater was investigated. The partition coefficient,  $K_{fs}$ , was calculated according to eq 1:

$$K_{fs} = \frac{V_s}{V_f \left( \frac{n_0}{n_f} - 1 \right)} \quad (1)$$

where  $V_s$  is the volume of the sample,  $n_f$  is the amount of the analyte extracted onto the sorbent at equilibrium,  $n_0$  is the initial amount of the analyte in the sample, and  $V_f$  is volume of the PIL on the thin film sheet. In this work,  $n_0$  was 17.5 ng for all individual PFASs included in this study and  $n_f$  values were obtained from extractions performed at equilibrium conditions by converting peak areas in mass extracted;  $V_f$  was 0.0028 mL.

Figure 4 shows the log  $K_{fs}$  values for 15 PFAS in ultrapure water and seawater, plotted against their log  $P$  values. In

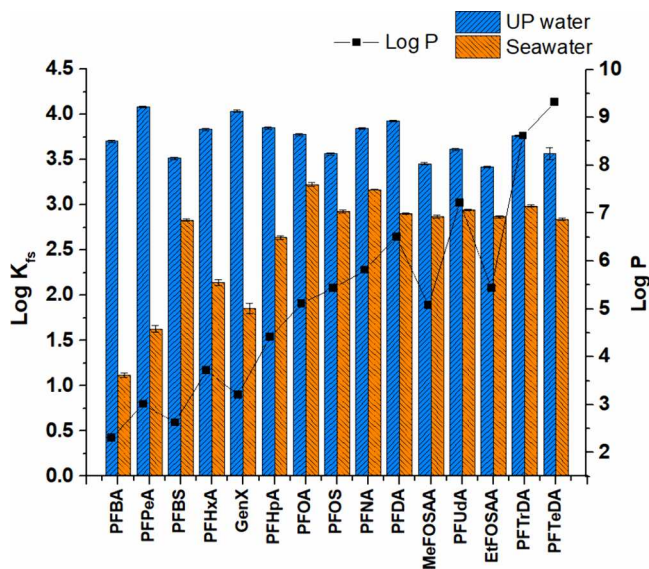


**Figure 4.** Plot of log  $K_{fs}$  in ultrapure water and simulated seawater and log  $P$  for the 15 PFAS investigated in this study. Extraction and desorption studies were performed at 90 min at an agitation speed of 1000 rpm.

ultrapure water, the extraction efficiencies for short- and long-chain PFAS are similar, indicating balanced extraction by the PIL TFME device. In seawater, competing ions reduce the efficiency of partitioning, particularly for short-chain PFAS (except PFBS), suggesting that electrostatic interactions govern their partitioning, which is affected by competing ions. Enrichment factors for all analytes ranged from 1.95 (MeFOSAA) to 2.57 (PFNA).

In this study, the van't Hoff equation (Supporting Information, Section 7) was used to further investigate the interaction mechanism governing the behavior of PFAS compounds on the PIL by extracting PFAS from ultrapure water at different temperatures (from 25 to 60 °C) for 150 min to ensure that equilibrium was reached for all analytes. Since the van't Hoff equation describes changes in the equilibrium constant of a chemical reaction with changes in temperature, the partition coefficients ( $K_{fs}$ ) of PFAS were calculated at different temperatures. The plots of ln  $K_{fs}$  versus temperature (Figure S7) showed a negative slope for all analytes, indicating that the thermodynamic process is endothermic, governed by ion-exchange interactions between the anionic PFAS and the PIL sorbent. This finding is consistent with previous findings,<sup>35,36</sup> which evaluated the ion-exchange mechanism between the free silanol groups on a pentafluorophenyl (PFP) stationary phase and positively charged analytes.

## METHOD VALIDATION

The PIL TFME devices were also assessed for suitability to quantitative analysis. The broad linear dynamic range achieved shows the great potential of the PIL to quantify low-, mid-, and high-concentration levels of PFAS. A lack-of-fit test was performed to assess the robustness of the linear regression. The significant  $F$  value ( $<0.0001$ ) was lower than 0.05 for all analytes, indicating that the model fits the data well (Table S5). The accuracy of the method (Table S6) was studied at 75, 300, 750, and 3000 ng L<sup>-1</sup> and over 7 days (Table S7). Good accuracy values, between 70% and 130%, were achieved at these levels, with precision  $<20\%$ . Figure S8 presents the calibration curves for the 15 analytes used to determine the LOQ values, which ranged from 1 to 10 ng L<sup>-1</sup> for all analytes except for PFPeA, which was 50 ng L<sup>-1</sup>. LODs for all analytes were 1 ng L<sup>-1</sup>, except for PFPeA.

The reusability of the PIL TFME is important, as it also demonstrates their robustness for routine analysis. Each tested PIL TFME device was used for approximately 20 extractions, with extraction efficiency variations ranging from 2% to 9% RSD across all analytes over the 20 uses (Figure S9).

## CONCLUSIONS

This study demonstrates the effectiveness of a PIL constituted by a IL monomer [ $C_9COOHVim^+$ ] [ $Br^-$ ] and cross-linker [ $C_{12}(Vim^+)_2$ ] $2[Br^-]$  for isolating and preconcentrating PFAS mixtures. Desorption studies showed that ammonium salts, particularly ammonium formate, are crucial for efficient removal of PFAS from the sorbent. pH and ionic strength studies revealed that shorter-chain PFAS were more affected by competing ions, while longer-chain PFAS showed a stable extraction performance. Calculated partition coefficients highlighted that the PIL sorbent efficiently extracted all 15 PFAS from ultrapure water and highlighted the impact of ionic strength, especially for short-chain PFAS. Kinetic studies indicated most PFAS reached equilibrium within 20–30 min, with the pseudo-second order model best describing the sorption process. Our results also indicate that the mechanism between the PIL sorbent and PFAS is an endothermic process, which is governed by ion-exchange interactions. Method validation confirmed the applicability of the PIL for quantitative analysis with LOQs from 1 to 50 ng L<sup>-1</sup>, although matrix-matched calibration for the quantification of PFAS in samples with high salinity is recommended. These results demonstrate the potential of PILs for a preconcentrated PFAS mixture and pave the way to further sorbent design strategies to improve the selectivity of the separation.

## ASSOCIATED CONTENT

### Supporting Information

The Supporting Information is available free of charge at <https://pubs.acs.org/doi/10.1021/acs.analchem.4c06522>.

Materials and reagents, preparation of the thin film devices, liquid chromatography and mass spectrometry conditions, preparation of the TFME for first use, kinetic models, PIL coating thickness, van't Hoff equation, tables and figures related to experiments in the manuscript (PDF)

## AUTHOR INFORMATION

## Corresponding Author

**Emanuela Gionfriddo** – Department of Chemistry and Biochemistry and Dr. Nina McClelland Laboratory for Water Chemistry and Environmental Analysis, The University of Toledo, Toledo, Ohio 43606, United States; Department of Chemistry, University at Buffalo, The State University of New York, Buffalo, New York 14260-3000, United States; [orcid.org/0000-0002-1836-1950](https://orcid.org/0000-0002-1836-1950); Email: [egionfri@buffalo.edu](mailto:egionfri@buffalo.edu)

## Authors

**Aghogho A. Olomukoro** – Department of Chemistry and Biochemistry and Dr. Nina McClelland Laboratory for Water Chemistry and Environmental Analysis, The University of Toledo, Toledo, Ohio 43606, United States; Department of Chemistry, University at Buffalo, The State University of New York, Buffalo, New York 14260-3000, United States

**Derek R. Eitzmann** – Department of Chemistry, Iowa State University, Ames, Iowa 50011, United States

**Jared L. Anderson** – Department of Chemistry, Iowa State University, Ames, Iowa 50011, United States; [orcid.org/0000-0001-6915-8752](https://orcid.org/0000-0001-6915-8752)

Complete contact information is available at:

<https://pubs.acs.org/10.1021/acs.analchem.4c06522>

## Author Contributions

**Aghogho A. Olomukoro**: Methodology, Formal analysis, Investigation, Visualization, Data curation, Writing—original draft. **Derek R. Eitzmann**: Methodology, Formal analysis, Investigation, Visualization, Data curation, Writing—review and editing. **Jared L. Anderson**: Conceptualization, Supervision, Writing—review and editing. **Emanuela Gionfriddo**: Conceptualization, Supervision, Project administration, Funding acquisition, Writing—review and editing.

## Notes

The authors declare no competing financial interest.

## ACKNOWLEDGMENTS

E.G. and A.A.O. acknowledge funding from the Environmental Chemical Science and Chemical Measurement and Imaging Programs at the National Science Foundation (CHE-2432184). J.L.A. and D.R.E. acknowledge funding from the Chemical Measurement and Imaging Program at the National Science Foundation (CHE-2203891). A.A.O. would like to thank Dr. Héctor Martínez-Pérez-Cejuela for his input on the manuscript. D.R.E. and J.L.A. thank the Alice Hudson Professorship at Iowa State University for support.

## REFERENCES

- Gionfriddo, E.; Souza-Silva, É. A.; Ho, T. D.; Anderson, J. L.; Pawliszyn, J. *Talanta* **2018**, *188* (June), 522–530.
- Ravelo-Pérez, L. M.; Hernández-Borges, J.; Asensio-Ramos, M.; Rodríguez-Delgado, M. A. *J. Chromatogr A* **2009**, *1216* (43), 7336–7345.
- Sha, C.; Yi-Sheng, Z.; Shui-Yuan, C.; Tian, Q.; Hao, S. *J. Sep. Sci.* **2011**, *34* (13), 1503–1507.
- Bahrololoomi Fard, S. M.; Ahmadi, S. H.; Hajimahmodi, M.; Fazaeli, R.; Amini, M. *Analytical Methods* **2020**, *12* (1), 73–84.
- Liu, J. F.; Jiang, G. B.; Chi, Y. G.; Cai, Y. Q.; Zhou, Q. X.; Hu, J. T. *Anal. Chem.* **2003**, *75* (21), 5870–5876.
- Trujillo-Rodríguez, M. J.; Nacham, O.; Clark, K. D.; Pino, V.; Anderson, J. L.; Ayala, J. H.; Afonso, A. M. *Anal. Chim. Acta* **2016**, *934*, 106–113.
- Qin, Z.; Bragg, L.; Ouyang, G.; Pawliszyn, J. *J. Chromatogr A* **2008**, *1196–1197* (1–2), 89–95.
- Pierola, I. F.; Agzenai, Y. *J. Phys. Chem. B* **2012**, *116* (13), 3973–3981.
- Zhang, K.; Kujawski, D.; Spurrell, C.; Wang, B.; Crittenden, J. C. *J. Environ. Sci. (China)* **2023**, *127*, 866–874.
- Cui, Q.; Pan, Y.; Wang, J.; Liu, H.; Yao, B.; Dai, J. *Environ. Pollut.* **2020**, *266*, 115330.
- Kotlarz, N.; McCord, J.; Collier, D.; Suzanne Lea, C.; Strynar, M.; Lindstrom, A. B.; Wilkie, A. A.; Islam, J. Y.; Matney, K.; Tarte, P.; Polera, M. E.; Burdette, K.; Dewitt, J.; May, K.; Smart, R. C.; Knappe, D. R. U.; Hoppin, J. A. *Environ. Health Perspect* **2020**, *128* (7), 1–12.
- Zarebska, M.; Bajkacz, S. *TrAC - Trends in Analytical Chemistry* **2023**, *163*, 117062.
- Dong, Q.; Min, X.; Huo, J.; Wang, Y. *Chem. Eng. J. Advances* **2021**, *7*, 100135.
- Chen, C.; Liang, X.; Wang, J.; Zou, Y.; Hu, H.; Cai, Q.; Yao, S. *J. Chromatogr A* **2014**, *1348*, 80–86.
- Eitzmann, D. R.; Anderson, J. L. *Anal. Chem.* **2024**, *96*, 11942.
- Eitzmann, D. R.; Varona, M.; Anderson, J. L. *Anal. Chem.* **2022**, *94* (8), 3677–3684.
- Cantoni, B.; Turolla, A.; Wellmütz, J.; Ruhl, A. S.; Antonelli, M. *Sci. Total Environ.* **2021**, *795*, No. 148821.
- Hansen, M. C.; Børresen, M. H.; Schlabach, M.; Cornelissen, G. *J. Soils Sediments* **2010**, *10* (2), 179–185.
- EPA. *EPA Method 537.1: Determination of Selected Per- and Polyfluorinated Alkyl Substances in Drinking Water by Solid Phase Extraction and Liquid Chromatography/Tandem Mass Spectrometry (LC/MS/MS)*; 2018; pp 1–50.
- Watson, R. *BMJ.* **2006**, *333* (7574), 873.
- Olomukoro, A. A.; DeRosa, C.; Gionfriddo, E. *Anal. Chim. Acta* **2023**, *1260*, No. 341206.
- Olomukoro, A. A.; Emmons, R. V.; Godage, N. H.; Cudjoe, E.; Gionfriddo, E. *J. Chromatogr A* **2021**, *1651*, No. 462335.
- Rodrigues, R. F.; Freitas, A. A.; Canongia Lopes, J. N.; Shimizu, K. *Molecules* **2021**, *26* (23), 7159.
- Amani, P.; Firouzi, M. *Colloids and Interfaces* **2022**, *6* (3), 41.
- Steffens, S. D.; Cook, E. K.; Sedlak, D. L.; Alvarez-Cohen, L. *Environ. Sci. Technol. Lett.* **2021**, *8* (12), 1032–1037.
- The Casual Analysis Team US EPA. *Causal Analysis/Diagnosis Decision Information System (CADDIS) Ionic Strength Overview*; <https://epa.gov/caddis/forms/contact-us-about-caddis>.
- Activity & Ionic Strength Activity vs. Concentration (Non-Ideal Solutions); <https://www.aqion.de/site/69>.
- Umeh, A. C.; Hassan, M.; Egbuatu, M.; Zeng, Z.; Al Amin, M.; Samarasinghe, C.; Naidu, R. *Sci. Total Environ.* **2023**, *904*, No. 166568.
- Kim, G.; Mengesha, D. N.; Choi, Y. *Sep. Purif. Technol.* **2024**, *349*, 127851.
- Zhang, Y.; Thomas, A.; Apul, O.; Venkatesan, A. K. *J. Hazard Mater.* **2023**, *460*, 132378.
- Hegaard, F.; Biro, R.; Ehtiati, K.; Thormann, E. *Langmuir* **2023**, *39* (4), 1456–1464.
- Du, Z.; Deng, S.; Bei, Y.; Huang, Q.; Wang, B.; Huang, J.; Yu, G. *J. Hazard Mater.* **2014**, *274*, 443–454.
- Son, H.; Kim, T.; Yoom, H. S.; Zhao, D.; An, B. *Water (Switzerland)* **2020**, *12* (11), 3287.
- Mohammadzadeh, F.; Golshan, M.; Haddadi-Asl, V.; Salami-Kalajahi, M. *Sci. Rep.* **2023**, *13* (1), 11900.
- Emmons, R. V.; Karaj, E.; Cudjoe, E.; Bell, D. S.; Tillekeratne, L. M. V.; Gionfriddo, E. *J. Chromatogr A* **2022**, *1685*, 463636.
- Bell, D. S.; Jones, A. D. *In Journal of Chromatography A* **2005**, *1073*, 99–109.